Sequential signaling in plasma-membrane domains during macropinosome formation in macrophages

Sei Yoshida[1], Adam D. Hoppe[1,2], Nobukazu Araki[3] and Joel A. Swanson[1,*]

[1]Department of Microbiology and Immunology, University of Michigan Medical School, Ann Arbor, MI 48109, USA
[2]Department of Chemistry and Biochemistry, South Dakota State University, Brookings, SD 57007, USA
[3]Department of Histology and Cell Biology, School of Medicine, Kagawa University, Miki, Kagawa 761-0793, Japan
*Author for correspondence (jswan@umich.edu)

Accepted 21 June 2009
Journal of Cell Science 122, 3250-3261 Published by The Company of Biologists 2009
doi:10.1242/jcs.053207

Summary

Macropinosomes are large endocytic vesicles that form in ruffling regions of plasma membrane. To analyze signal organization relative to ruffle closure into circular ruffles and cup closure into macropinosomes, this study used quantitative microscopy to measure 3′ phosphoinositides and small-GTPase activities in a representative subset of forming macropinosomes. Macropinocytosis was stimulated by the addition of macrophage colony-stimulating factor (M-CSF) to macrophages expressing fluorescent reporter proteins. Ratiometric and fluorescence resonance energy transfer (FRET) microscopy determined that Rac1 activity and phosphatidylinositol (3,4,5)-trisphosphate [PtdIns(3,4,5)P_3] levels increased transiently, peaking 26-30 seconds after ruffle closure. Three-dimensional reconstruction of cells labeled with the fluorescent dye FM4-64 showed that PtdIns(3,4,5)P_3 was restricted to open, circular cups in the plasma membrane. Quantitative fluorescence microscopic methods determined the timing of cup closure, which followed 40-100 seconds after Rac1 and PtdIns(3,4,5)P_3 deactivation and coincided with accumulation of phosphatidylinositol 3-phosphate and Rab5a. Thus, ruffle closure creates a circular domain of plasma membrane that localizes the activation and deactivation of Rac1 and phosphoinositide 3-kinase (PI3K), followed by recruitment of Rab5a and the contractile activities of cup closure.

Supplementary material available online at
http://jcs.biologists.org/cgi/content/full/122/18/3250/DC1

Key words: Macropinocytosis, Macrophage, PtdIns(3,4,5)P_3, Rac1, FRET

Introduction

Macropinocytosis is an endocytic process that internalizes relatively large portions of plasma membrane. When macrophages or epithelial cells are stimulated with growth factors or phorbol esters, cell-surface membrane ruffles constrict at their distal margins into macropinocytic vesicles, which can exceed 5.0 μm diameter (Swanson, 1989; Racoosin and Swanson, 1989; Hewlett et al., 1994). Macropinocytosis contributes significantly to immunity and infection because it is used for major histocompatibility complex (MHC) class-I and class-II antigen presentation and is an infectious entry pathway for pathogenic bacteria and viruses (reviewed by Norbury, 2006; Kerr and Teasdale, 2009; Mercer and Helenius, 2009).

Macropinosome formation begins with membrane-ruffle formation. Ruffles are actin-rich, sheet-like extensions of cell membrane, distributed over the dorsal surfaces of cells that adhere to flat surfaces. Some ruffles change to curved, or C-shaped, sheets, which close to form circular, O-shaped cups of plasma membrane that then separate by membrane scission into intracellular macropinosomes. Thus, two closure activities characterize macropinosome formation: ruffle closure (the transition from curved ruffles to circular ruffles) and cup closure (the process that separates nascent macropinosomes from plasma membrane) (Swanson, 2008).

Membrane phosphoinositides are essential for macropinosome formation. In macrophages, inhibitors of phosphoinositide 3-kinase (PI3K) block the process of macropinosome formation without reducing curved-ruffle formation (Araki et al., 1996; Araki et al., 2003). Moreover, GFP-BtkPH, which binds to phosphatidylinositol (3,4,5)-trisphosphate [PtdIns(3,4,5)P_3] when expressed in living cells (Varnai et al., 1999), is recruited to macropinosomes in human epidermoid carcinoma cells (Araki et al., 2007), suggesting a role for PtdIns(3,4,5)P_3 in cup closure. Also, fluorescent PLC-PH domains, which bind to phosphatidylinositol (4,5)-bisphosphate [PtdIns(4,5)P_2] (Varnai and Balla, 1998), and FYVE domains, which bind to phosphatidylinositol 3-phosphate [PtdIns(3)P] (Kutateladze et al., 1999; Gillooly et al., 2000), are recruited to membrane ruffles and forming macropinosomes in human epidermoid carcinoma cells (Araki et al., 2006; Araki et al., 2007).

Small GTPases also contribute to macropinosome formation. Ruffling responses to macrophage colony-stimulating factor (M-CSF) are reduced in Rac1-deficient macrophages (Wells et al., 2004) or by overexpression of dominant-negative Rac1 (Cox et al., 1997). The Rac1-binding protein WAVE2 is crucial for ruffling and motility responses to stimulation by M-CSF (Kheir et al., 2005), suggesting that M-CSF-induced macropinocytosis is Rac1- and WAVE2-dependent. GTP-bound Rac1 and Cdc42 can also activate p21-activated kinase-1 (PAK-1), which regulates macropinocytosis (Dharmawardhane et al., 2000), possibly through phosphorylation of Ctb (also known as BARS) (Liberali et al., 2008). Additionally, microinjection of dominant-negative Rac1 into immature dendritic cells does not eliminate membrane ruffles (West et al., 2000), which suggests that Rac1 instead organizes the transformation of membrane ruffles into macropinosomes. RhoG activates Rac1 (Katoh and Negishi, 2003) and might stimulate macropinocytosis via Rac1. Roles for Cdc42 and Arf6 in macropinosome formation have also been suggested (Garrett et al., 2000; West et al., 2000); overexpression of dominant-negative Arf6 in bone-marrow-derived (BM)-macrophages reduces M-CSF-stimulated membrane ruffling

(Zhang et al., 1999). Roles for Ras and Rab5 during macropinocytosis have also been demonstrated (Bar-Sagi and Feramisco, 1986; Li et al., 1997; Lanzetti et al., 2004). The Rab5 effector Rabankyrin-5 localizes to macropinosomes and might contribute to their formation or stabilization (Schnatwinkel et al., 2004).

The intermittent and spontaneous formation of macropinosomes in macrophages at various times after exposure to M-CSF indicates that macropinosomes are self-organized structures whose morphogenesis is triggered, but not guided, by receptor activation. M-CSF receptors are likely to be both inside and outside of the forming macropinosomes, which would make it difficult for the structures themselves to be shaped by the distribution of activated receptors. Rather, regions of the cortex must organize into domains of membrane with localized actin polymerization and oriented contractile activities that close circular ruffles into discrete intracellular vesicles. This prompts questions regarding how the sequence of morphological changes is regulated.

Quantitative analysis of this regulation is complicated by the variability of timing and macropinosome sizes. Here, we defined a morphological framework for macropinosome formation, and investigated corresponding patterns of PtdIns(3,4,5)P_3, PtdIns(3)P and GTPase recruitment and activation in a representative subset of macropinosomes, relative to the stages of macropinosome formation. Rac1 activation and PtdIns(3,4,5)P_3 generation occurred transiently within the circular domain of plasma membrane formed by ruffle closure. Rab5a recruitment and PtdIns(3)P generation began shortly after deactivation of Rac1 and PtdIns(3,4,5)P_3, and coincided with closure of the cup into a macropinosome. These results indicate that sequential signaling for macropinosome formation occurs in a cup-shaped domain of plasma membrane, which is defined by ruffle closure.

Results

A quantitative model of macropinosome formation

To study quantitatively the role of phosphoinositides and small-GTPase signals during macropinosome formation, we first analyzed the morphology of macropinocytosis in time-lapse, phase-contrast images of BM-macrophages. The addition of M-CSF to BM-macrophages induced cell spreading and membrane ruffling, followed by sporadic formation of macropinosomes. Fig. 1A shows the sequence of events characteristic of macropinosome formation. A membrane ruffle (Fig. 1A; +0 seconds) enlarged and bent into a curved ruffle (+60 seconds) then closed into a circular, cup-shaped ruffle (+120 seconds). The cup remained stationary for about 80 seconds (+120 to +200 seconds), then moved towards the center of the cell (+220 seconds). We designated four stages of macropinosome formation on the basis of these morphologies. The ‘irregular ruffle’ stage consists of a membrane ruffle before it assumes a curved profile. The ‘curved ruffle’ stage is the period in which a ruffle adopts a C-shape. In ruffle closure, the curved ruffle becomes an O-shaped circular cup, or circular ruffle. This ‘circular ruffle’ stage is the period from ruffle closure to the first movement of the macropinosome away from the cell margin. Closure of the circular ruffle into a macropinosome probably occurs sometime during this stage. Centripetal movement begins the ‘motile’ stage. In a previous paper (Araki et al., 2003), we used the term ‘circular ruffle’ to describe what we refer to here as a curved ruffle. Our new distinction between curved and circular ruffles was prompted by the pronounced signaling associated with the transition between these two stages (see below).

We then characterized the sizes of macropinosomes and the timing of the morphological stages. The duration of each stage and the diameters of the resulting macropinosomes were measured just after their closure into phase-bright vesicles. For 65 recorded macropinosomes larger than 0.8 μm, the mean diameter was 1.75±0.60 μm (Fig. 1B), which was similar to the dimensions described in earlier studies (Swanson, 1989; Racoosin and Swanson, 1989). Macropinosomes formed stochastically following M-CSF stimulation with a right-skewed frequency distribution that could be described by a log-normal- or a γ-distribution (Fig. 1C). The time spent in each stage was highly variable (Fig. 1D). By calculating the Pearson product-moment correlation coefficients (R), we did not identify significant correlations between durations of the various stages and macropinosome size. However, there was a significant positive correlation between macropinosome size and the time from M-CSF addition to the end of the circular stage (R=0.39, P<0.05). This correlation might reflect a contribution of cell spreading to macropinosome size. Given the stochastic nature of the four stages, we restricted our analyses of signaling to a limited but representative size-range of macropinosomes (1.2- to 2.2-μm diameter). Within this subset, we also observed a consistent duration of the curved stage: 22 of the 41 representative macropinosomes had a 60-second curved stage (Fig. 1D). Therefore, to facilitate quantitative comparisons of signal timing relative to the stages of macropinosome formation, we concentrated on the 1.2- to 2.2-μm macropinosomes with a 60-second curved stage (Fig. 1E). Our objective was to delineate the timing of signals relative to ruffle closure, when C-shaped ruffles become O-shaped ruffles, and cup closure, when the nascent macropinosome becomes isolated from the plasma membrane (Fig. 1F).

Rac1, Rac2 and Cdc42 signals during macropinosome formation

Because Rac1, Rac2 and Cdc42 are activated on forming phagosomes (Hoppe and Swanson, 2004), we hypothesized that these small GTPases would be recruited during macropinosome formation. Ratiometric fluorescence (RF) microscopy of a YFP chimera of a p21-binding domain (PBD) from Pak1 was used to localize GTP-bound forms of endogenous Rac1, Rac2 or Cdc42 (Hoppe and Swanson, 2004). We detected some selective recruitment of yellow fluorescent protein (YFP)-PBD to spreading lamellipodia and ruffles, especially just after the addition of M-CSF; this indicated weak activation of Rac1, Rac2 or Cdc42 (Fig. 2A; supplementary material Movie 1). After this initial response, however, YFP-PBD:CFP ratios increased locally in forming macropinosomes, beginning in the circular stage (80 seconds) and then returning to baseline levels within 60 seconds (Fig. 2A). To quantify the activation of small GTPases in these images, we divided the ratio of YFP-PBD:CFP on the macropinosome by the ratio for the entire cell. YFP:CFP ratios were measured for the region of cytoplasm forming the macropinosome (R_{mac}=ratio of macropinosome) and for the entire cell (R_{cell}=ratio of cell). The ratio of these ratios provided the relative concentration of YFP chimera; R_{mac}/R_{cell}>1.0 indicated YFP-PBD recruitment to macropinosomes. The resulting traces were aligned by setting the beginning of the curved stage in each plot as time=0. For this subset of the data, curved ruffles closed into circles at 60 seconds. These recruitment indexes increased at 80 seconds in all samples and remained high for 40-60 seconds (Fig. 2C), indicating that some combination of Rac1, Rac2 or Cdc42 was activated briefly at the beginning of the circular stage.

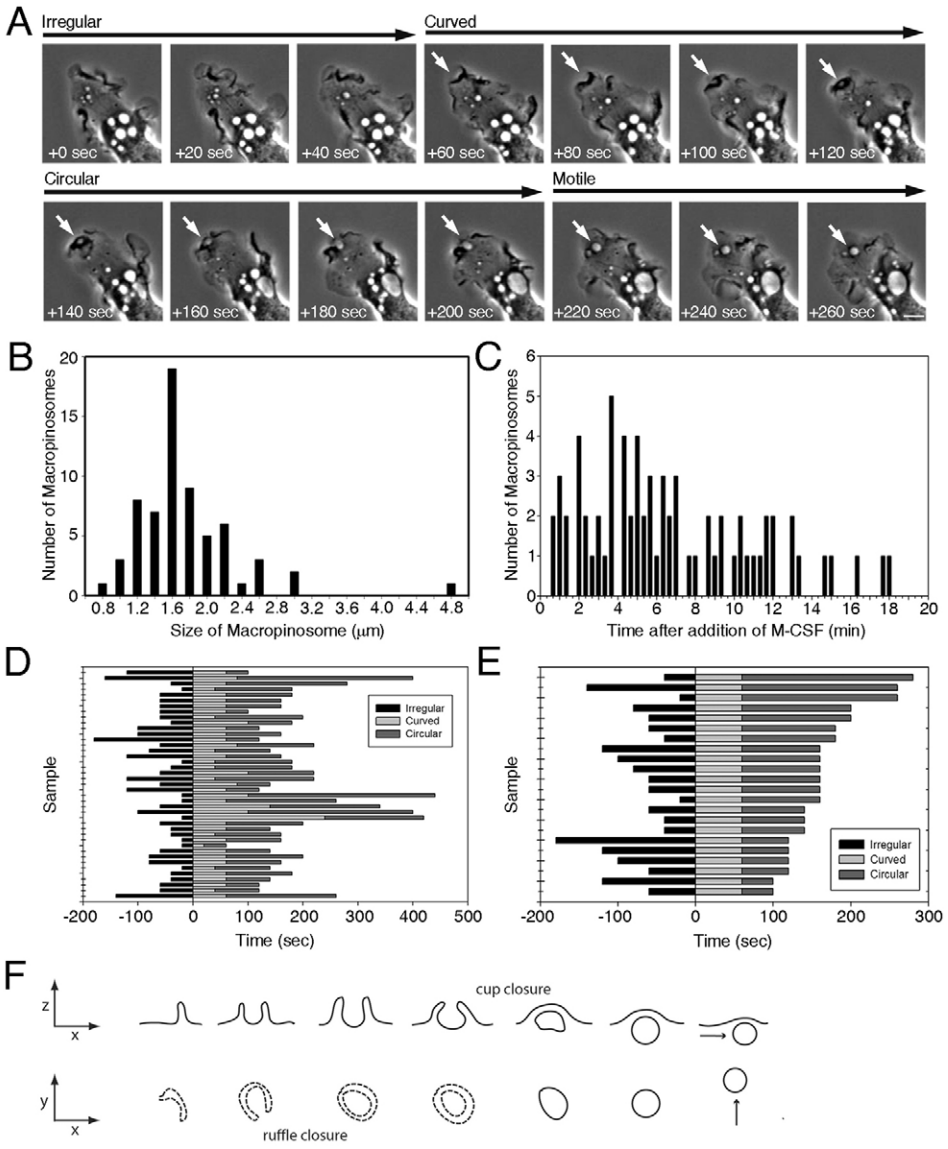

Fig. 1. A quantitative model of macropinosome formation. (A) Typical phase-contrast images of macropinosome formation (white arrows). Irregular ruffles were phase-dense bands at the periphery of the cells (+0 sec to +40 sec), which changed into curved ruffles (+60 sec). A curved ruffle (white arrow) closed into a circular ruffle (+120 sec), then moved centripetally after a 100-second pause (+220 sec). These morphological transitions were divided into four stages of macropinosome formation: irregular, curved, circular and motile. Scale bar: 3 μm. (B) The size distribution of 65 macropinosomes, defined as the diameter at the first frame of the circular ruffle stage. (C) The frequency of macropinosome formation. The *x*-axis indicates the time of the beginning of the curved stage, relative to the addition of M-CSF. (D) Macropinosomes in the size range of 1.2- to 2.2-μm diameter were analyzed (n=41), with the beginning of the curved stage set to 0 seconds. (E) The subset of macropinosomes used to evaluate signaling (1.2-2.2 μm, 60-second curved-ruffle stage). The beginning of the curved-ruffle stage was set as time=0. (F) Diagram of the two stages of macropinosome closure. The top row shows a side view and the bottom row shows a top view (as observed in the microscope, A) of plasma membrane and macropinosome membranes. Ruffle closure is the formation of a complete circular ruffle, comprised entirely of plasma membrane; ruffle closure marks the beginning of the circular stage. Cup closure marks the separation of the macropinosome from the plasma membrane sometime after ruffle closure.

Recruitment of small GTPases was measured by RF microscopy of macrophages expressing soluble CFP and YFP-chimeras of Rac1, Rac2 or Cdc42. Unexpectedly, ratio images of YFP-Rac1:CFP, YFP-Rac2:CFP and YFP-Cdc42:CFP indicated that their localization to macropinosomes was only slightly greater than on other regions of the plasma membrane (data not shown).

Given the patterns of activation indicated by YFP-PBD, we next examined activation of Rac1, Rac2 and Cdc42 using fluorescence resonance energy transfer (FRET) stoichiometry, an analytical imaging method that can quantify interactions between separately expressed fluorescent proteins inside cells (Hoppe et al., 2002). To determine the activation profiles of the component GTPases, we expressed CFP-PBD plus YFP-Rac1, YFP-Rac2 or YFP-Cdc42, then collected images after stimulation with M-CSF and analyzed the images by FRET stoichiometry. Following collection of CFP, YFP and FRET images, image processing for FRET stoichiometry generated three images: E_A, E_D and R_M. E_A is proportional to the fraction of YFP-chimera in complex with CFP-PBD. YFP-Rac1 was activated briefly at the cell margins immediately after the addition of M-CSF, then it was activated transiently in forming macropinosomes at the beginning of the circular stage (supplementary material Movie 2). In particular, E_A increased at the end of the curved stage and remained elevated for 20-60 seconds (Fig. 2B). The cumulative data from ten time-course image series indicated that E_A increased at 60 seconds, peaked at 90±14 seconds (30±14 seconds after ruffle closure) and returned to basal levels between 120 and 140 seconds (Fig. 2D). The same imaging strategy indicated that YFP-Rac2 and YFP-Cdc42 were not activated during macropinosome formation, despite the fact that YFP-Cdc42 activation is detected in forming phagosomes (Hoppe et al., 2008) and in lamellipodia (data not shown). Similar Cdc42 activation patterns were observed by RF microscopy of cells expressing CFP and YFP-CBD, the Cdc42-binding domain of WASP (data not shown). It remains possible that Cdc42 is activated in only the distal margins of curved and circular ruffles, and that significant FRET signals from YFP-Cdc42 and CFP-PBD were either out-of-focus or undetectable. However, overall, these results indicate that Rac1 was activated selectively after ruffle closure, consistent with Rac1 activity facilitating closure of the cup into a macropinosome.

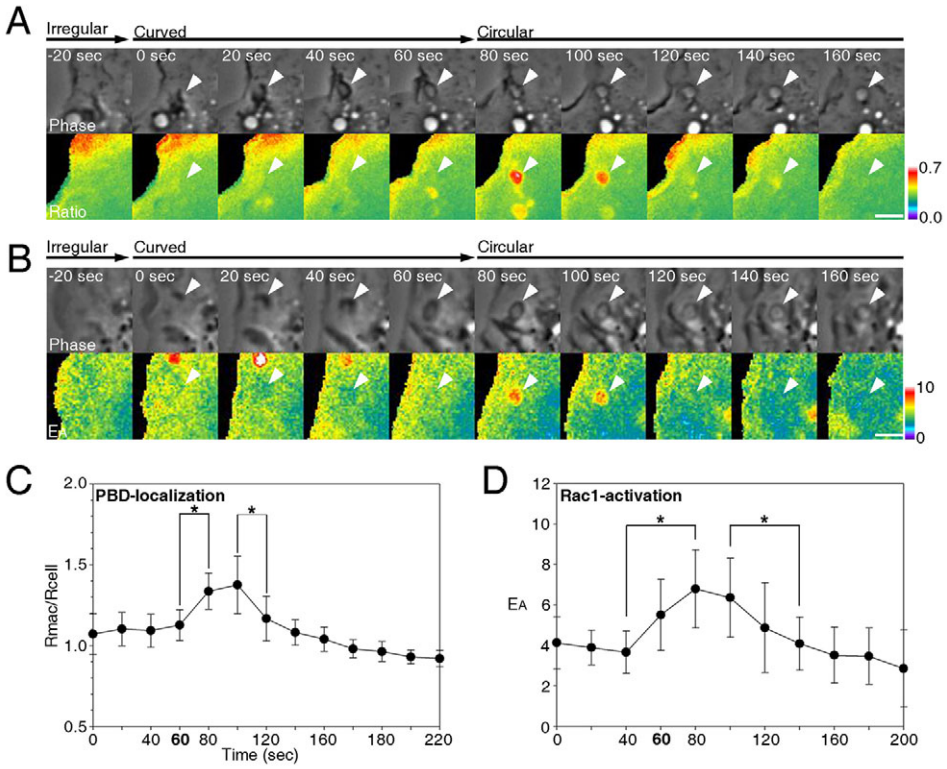

Fig. 2. Rac1 dynamics in macropinocytic cups. (A) Ratiometric imaging of YFP-PBD and CFP. Phase-contrast (Phase) and ratiometric (Ratio) images of BM-macrophages expressing YFP-PBD with soluble CFP during macropinosome formation. '0 sec' marks the beginning of the curved stage. Scale bar: 3 µm. Color bars indicate the molar ratio of YFP-PBD:CFP. The ratio of YFP-PBD:CFP at the area of macropinosome formation increased at 80 seconds. Arrowheads indicate a forming macropinosome. (B) FRET stoichiometry imaging of YFP-Rac1 activation during macropinosome formation. Phase-contrast (Phase) and E_A images of a BM-macrophage expressing YFP-Rac1 and CFP-PBD. E_A is proportional to the fraction of Rac1-YFP bound to PBD-CFP. E_A values were high at 80 and 100 seconds. Scale bar: 3 µm. Color bars indicate values in the E_A images. (C) Plots of average R_{mac}:R_{cell}, indicating the dynamics of YFP-PBD localization on macropinosomes (n=10). The differences between the localization index of YFP-PBD at 60 and 80 seconds (*P<0.001) and at 100 and 120 seconds were significant (*P<0.001). Error bars indicate standard deviation. (D) Plots of average E_A values on macropinosomes (n=10). The differences between the values at 40 and 80 seconds and also 100 and 140 seconds were significant (*P<0.001), indicating that Rac1 was activated at areas of macropinosome formation from 60 to 100 seconds. Error bars indicate standard deviation.

Generation of PtdIns(3,4,5)P_3 during macropinosome formation

Previous studies reported that PtdIns(3,4,5)P_3 and PtdIns(3)P localize to macropinosomes in human epidermoid carcinoma cells (Araki et al., 2006; Araki et al., 2007) and that PI3K-inhibitor-treated macrophages make circular ruffles that recede without closing into macropinosomes (i.e. ruffle closure without cup closure) (Araki et al., 1996; Araki et al., 2003). These studies suggested therefore that 3′ phosphatidylinositols regulate the contractile activities of cup closure. Accordingly, we expected that local concentrations of PtdIns(3,4,5)P_3 would increase on unclosed macropinocytic cups. The distributions of PtdIns(3,4,5)P_3 were monitored using RF microscopy of cells expressing CFP and YFP-BtkPH, which binds to PtdIns(3,4,5)P_3 (Varnai et al., 1999). Ratiometric images calculated from cells expressing YFP-BtkPH and CFP represented the molar ratio of YFP-BtkPH to soluble CFP at each pixel in the image (Henry et al., 2004; Hoppe et al., 2004). Following the addition of M-CSF, YFP-BtkPH:CFP ratios increased transiently in lamellipodia and the first ruffles that formed (Fig. 3A; supplementary material Movie 3). However, subsequent ruffling showed reduced PtdIns(3,4,5)P_3 activity; rather, PtdIns(3,4,5)P_3 was largely restricted to forming macropinosomes. YFP-BtkPH:CFP ratios increased dramatically just after ruffle closure (Fig. 3A; +60 to +80 seconds), indicating localized PtdIns(3,4,5)P_3 generation at the beginning of the circular stage. In eight out of the ten image series, the peak of the localization index for YFP-BtkPH occurred at 80 seconds and dropped quickly to baseline (Fig. 3B,C). Therefore, PtdIns(3,4,5)P_3 was generated transiently on macropinosomes at the beginning of the circular stage, just after ruffle closure. We refer to this hereafter as the PtdIns(3,4,5)P_3 spike.

To ensure that the PtdIns(3,4,5)P_3 spike was not an artifact of increased membrane density in circular ruffles, we normalized the YFP-BtkPH fluorescence to membrane distributions. To mark plasma membranes during macropinosome formation, we expressed CFP containing the N-terminal palmitoylation sequence from neuromodulin (CFP-MEM). Expression of CFP-MEM provides a method to label plasma membrane and newly formed macropinosomes (Araki et al., 2007). We reasoned that the fluorescence of CFP-MEM in the region of a forming macropinosome should increase as the distal margin of the open cup doubles over to form a vesicle. BM-macrophages expressing YFP-BtkPH and CFP-MEM were imaged at 3-second intervals (Fig. 3D). The accumulation of PtdIns(3,4,5)P_3 in the plasma membrane began within 10 seconds of ruffle closure and seemed to be restricted to the inner membrane of the macropinocytic cup. These results

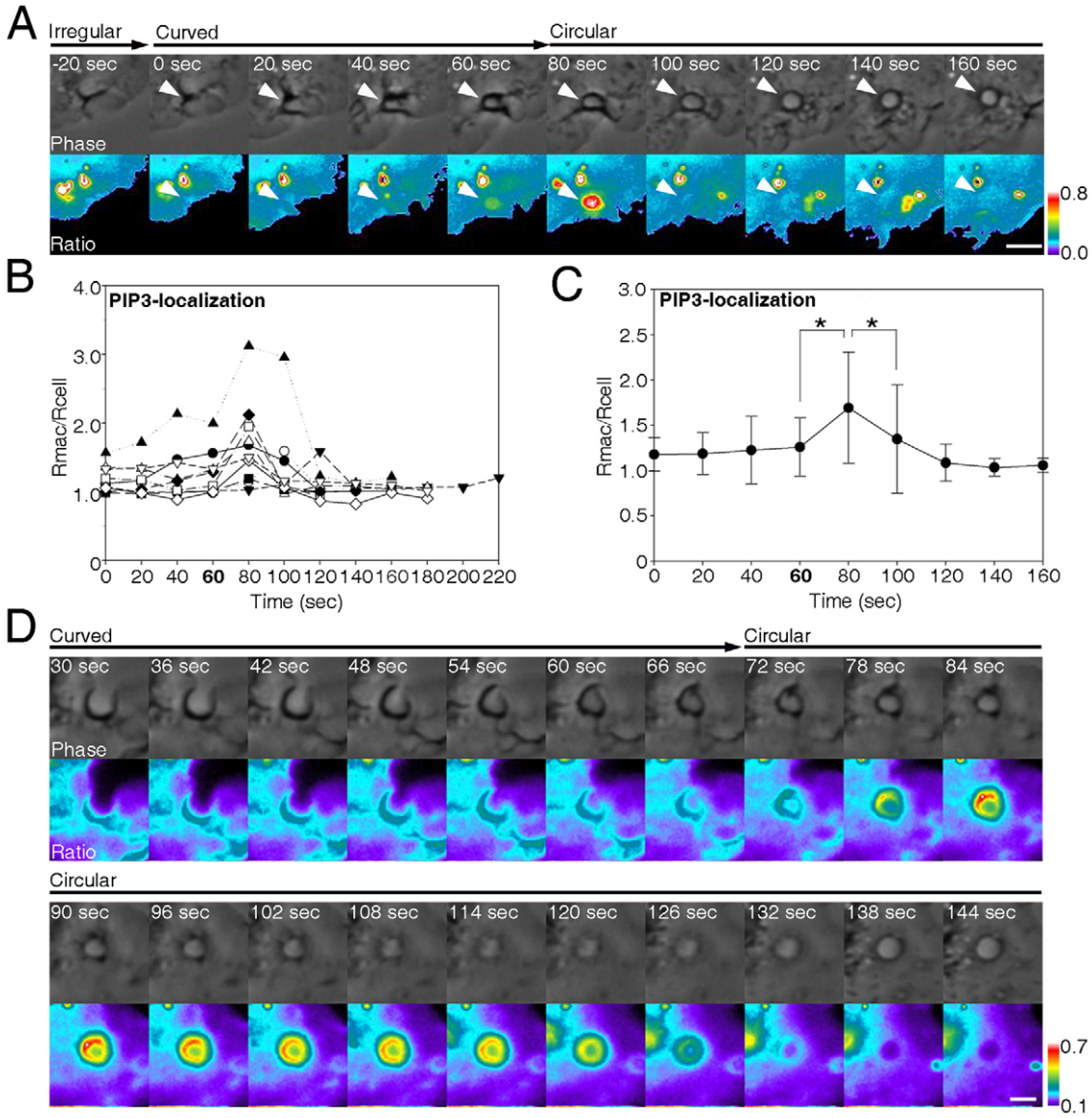

Fig. 3. PtdIns(3,4,5)P_3 dynamics during macropinosome formation. (A) Phase-contrast (Phase) and ratiometric (Ratio) images of macropinosome formation in BM-macrophages expressing YFP-BtkPH and CFP. Indicated times are relative to the beginning of the curved-ruffle stage. Arrowheads indicate a forming macropinosome. Color bars indicate the molar ratio of YFP-chimera:CFP in the ratio images. The YFP-BtkPH:CFP ratios increased at 60 and 80 seconds and returned to baseline at 100 seconds. Scale bar: 4 µm. (B) Plots of R_{mac}:R_{cell} in six cells, indicating the dynamics of YFP-BtkPH on macropinosomes. 60 seconds marks the end of the curved-ruffle stage (i.e. ruffle closure). YFP-BtkPH localization increased transiently after 60 seconds. (C) Plot of average R_{mac}:R_{cell}. The differences between the localization indices of YFP-BtkPH at 60 and 80 seconds (*P<0.01) and also that at 80 and 100 seconds were statistically significant (*P<0.05), indicating that PtdIns(3,4,5)P_3 (PIP3) was transiently generated after 60 seconds. Error bars indicate standard deviation. (D) The dynamics of a PtdIns(3,4,5)P_3 spike in a macrophage expressing YFP-BtkPH and CFP-MEM. Images were collected every 3 seconds; 6-second intervals are depicted. PtdIns(3,4,5)P_3 concentrations in the plasma membrane began to increase shortly after ruffle closure (66 sec). Scale bar: 1 µm.

suggested that PtdIns(3,4,5)P_3 accumulation in response to M-CSF was conditional on ruffle closure. In support of this, the transient PtdIns(3,4,5)P_3 generation beginning after ruffle closure was evident in macropinosomes of all sizes (n=15, 1.0- to 2.2-µm diameter, data not shown). For events in which the start of the curved phase was set to zero, there was a strong correlation between the start of the circular stage and the transient accumulation of YFP-BtkPH (R=0.90, P=2×10^{-6}), whereas the start of the motile phase was uncorrelated with the start of the circular phase (data not shown). This strong correlation indicated that PtdIns(3,4,5)P_3 amplification required ruffle closure.

The PtdIns(3,4,5)P_3 spike occurs in open cups

These results indicated that PtdIns(3,4,5)P_3 accumulation in circular ruffles precedes cup closure, which is consistent with previous studies showing that PI3K-inhibitor-treated macrophages make circular ruffles that recede without closing into macropinosomes (Araki et al., 1996; Araki et al., 2003). If elevated concentrations of PtdIns(3,4,5)P_3 organize the contractile activities of cup closure, then the PtdIns(3,4,5)P_3 signal should be restricted to the membranes of the circular ruffle. We therefore examined the localization of the PtdIns(3,4,5)P_3 spike relative to the cup shape.

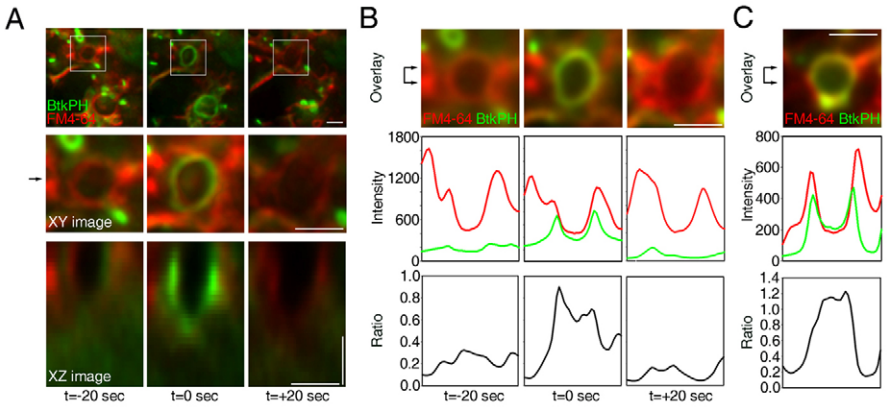

Fig. 4. The PtdIns(3,4,5)P_3 spike was restricted to the inside of the circular ruffle. Macropinosome formation in macrophages expressing YFP-BtkPH in the presence of FM4-64 dye was observed in 3D reconstructions. Complete *z*-axis image stacks were collected every 20 seconds, then the image series were deconvolved to observe PtdIns(3,4,5)P_3 spikes in three dimensions. Red and green in each panel indicate the localization of FM4-64 and YFP-BtkPH, respectively. Scale bars: 2 µm. (A) 3D image reconstruction of a PtdIns(3,4,5)P_3 spike. Top panels are *xy*-projections of reconstructed cell images. Squares in the top panels indicate the macropinosome areas that are enlarged in the corresponding middle panels. Bottom panels are *xz*-images of the areas indicated by the arrow in the middle panels. YFP-BtkPH fluorescence appeared transiently in the circular ruffle at *t*=0 seconds. (B) Quantitative analysis of fluorophore distributions. Deconvolved images were compressed to display total signal intensities along the *z*-axis (top panels). Resulting images were line-scanned along the *x*-axis through the center of the macropinosome (bracket-shaped arrow of top panels) and corresponding intensities along the *x*-axis were plotted in the middle panels. On the basis of these traces, ratios of YFP-BtkPH fluorescence to FM4-64 fluorescence were calculated (bottom panels). Comparing the middle and bottom panels indicates that the increased ratios at *t*=0 seconds were restricted to the membrane between the two peaks (green line) of the FM4-64 curve. (C) Another PtdIns(3,4,5)P_3 spike on a deconvolved and overlaid image (top panel), with fluorescence intensities line-scanned along the *x*-axis through the center of the cup. The *x*-axis corresponds with the position of the bracket-shaped arrow in the top panels. The ratio of YFP-BtkPH to FM4-64 fluorescence was calculated (bottom panels). High ratio values were restricted to the membrane between the two peaks of the FM4-64 curve (green line).

Time-lapse three-dimensional (3D)-reconstruction microscopy was used to observe distribution patterns of PtdIns(3,4,5)P_3 within macropinocytic cups. Cells expressing YFP-BtkPH were observed in the presence of FM4-64, a lipophilic dye that preferentially labels exposed membranes. Image *z*-stacks were acquired at 20-second intervals after addition of M-CSF. Each image *z*-stack was deconvolved to recover the 3D distributions of PtdIns(3,4,5)P_3 relative to plasma membrane. The top panels of Fig. 4A show *xy*-dimension images of a reconstructed cell at three time points, revealing two peaks of YFP-BtkPH fluorescence at *t*=0 seconds. The middle and bottom rows of Fig. 4A are *xy* and *xz* projections, respectively, of the reconstructed cup (from squares of top panels). As expected, PtdIns(3,4,5)P_3 was distributed along the inside of the open cup at *t*=0 seconds, suggesting that PtdIns(3,4,5)P_3 amplification was restricted to the inner membrane (Fig. 4A, bottom panels). To quantify this result, we measured the YFP-BtkPH signal intensity relative to the plasma-membrane distribution (Fig. 4B,C). Because of membrane folding at sites of ruffles, the intensity of FM4-64 signal at circular ruffles was expected to be higher than in flat areas of the cell surface. Deconvolved cell images were overlaid and FM4-64 and YFP-BtkPH signals were line-scanned along the *x*-axis through the center of macropinosome (Fig. 4B, bracket with arrowheads). The FM4-64 intensity curves corresponded to the *xy* images, indicating high plasma-membrane densities in the circular ruffles (Fig. 4B, red lines in middle panels). YFP-BtkPH curves indicated that the intensity increased only at *t*=0 seconds (Fig. 4B, green line in middle panels). Comparing the red and green curves indicated that the increase of YFP-BtkPH at *t*=0 seconds was restricted to the inside of the cup. To normalize the intensity of the YFP-BtkPH signals relative to plasma-membrane distributions, we calculated the ratio of YFP-BtkPH to FM4-64 fluorescence (Fig. 4B, bottom panels). The curves indicated that the highest ratio values were between the two peaks of the FM4-64 curve, indicating that the concentration of PtdIns(3,4,5)P_3 was elevated inside of the cup. The uniformly high ratio inside of the cup was also observed on another macropinosome (Fig. 4C). These data demonstrate that PtdIns(3,4,5)P_3 amplification was restricted to the membrane of the circular ruffle, possibly the inner membrane of the cup. This is consistent with studies in *Dictyostelium discoideum*, which localized uniformly high concentrations of PtdIns(3,4,5)P_3 in macropinocytic cups (Mercanti et al., 2006).

The PtdIns(3,4,5)P_3 spike is completed prior to cup closure

The timing of cup closure was measured by two methods. Co-expression of YFP-BtkPH and CFP-MEM allowed visualization of both the PtdIns(3,4,5)P_3 spike and the increase of membrane fluorescence that accompanied membrane doubling during cup closure. We reasoned that cup closure should be identifiable as the time when membranes have fully doubled over and CFP-MEM fluorescence reaches maximal values (Fig. 5A). As shown in Fig. 5B, the spike of YFP-BtkPH fluorescence at 20 seconds after ruffle closure was followed by a gradual increase in the fluorescence of CFP-MEM, which reached a maximal value 100 seconds after ruffle closure (Fig. 5B, middle panels, red arrowhead). Measurements of the time to maximal CFP-MEM fluorescence in ten macropinosomes showed consistent delays relative to the PtdIns(3,4,5)P_3 spike and indicated that cup closure occurred more than 60 seconds after the PtdIns(3,4,5)P_3 spike (Fig. 5C; supplementary material Table S1).

As an independent measure of cup closure, we quantified the depletion of FM4-64 fluorescence inside closed macropinosomes. FM4-64 exhibits low fluorescence in water and high fluorescence upon binding the plasma membrane, allowing observation of FM4-64-labeled membrane in dye-containing medium. The binding is rapid and reversible, and fluorescence is easily photobleached. We predicted that the FM4-64 fluorescence in closed macropinosomes

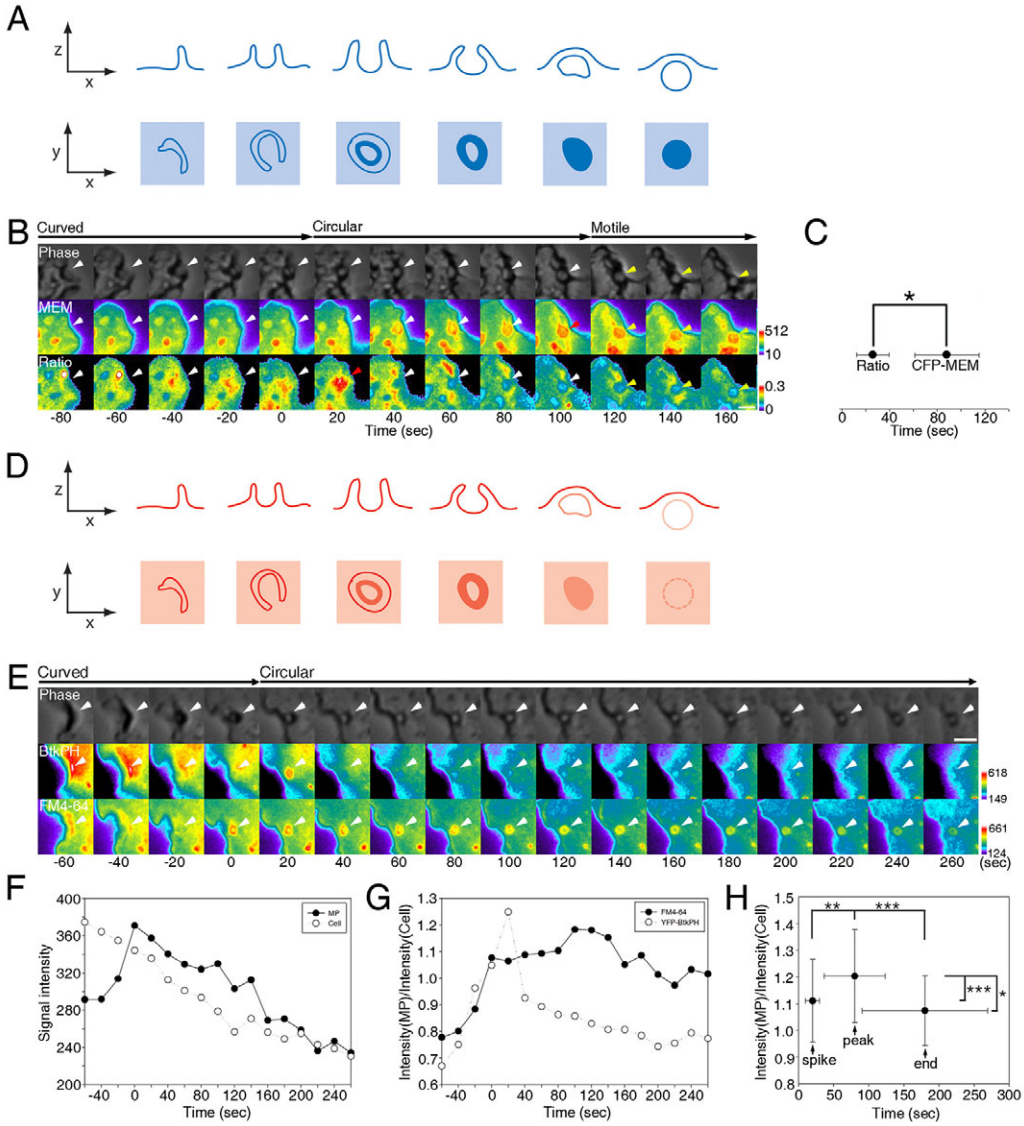

Fig. 5. The PtdIns(3,4,5)P_3 spike precedes cup closure. (A) Strategy for identifying the point of cup closure using CFP-MEM-labeled membranes. The top row shows the arrangements of plasma membrane on the top of the cell during macropinosome formation. The bottom row shows the corresponding fluorescence intensity of CFP-MEM during ruffling and macropinosome formation. Fluorescence intensities should increase as the membrane doubles over, reaching maximal values at the point of cup closure. (B) Macropinosome formation in macrophages expressing YFP-BtkPH and CFP-MEM. Arrowheads indicate a forming macropinosome. The top row shows phase-contrast images of the stages of macropinosome formation. The middle row shows the relative density of membrane, as indicated by the intensity of the CFP-MEM images. CFP-MEM fluorescence in the macropinosome increased during the circular stage, indicative of membrane doubling and cup closure. The bottom row shows the YFP-BtkPH:CFP-MEM ratio, which indicates the spike of PtdIns(3,4,5)P_3 concentration in membranes just after ruffle closure (red arrowhead). Scale bar: 3 μm. Color bars indicate the signal intensity of CFP-MEM or the molar ratio of YFP-BtkPH:CFP-MEM in each image. (C) Timing of the peak values for YFP-BtkPH:CFP-MEM ratios and CFP-MEM fluorescence, relative to ruffle closure (t=0 seconds), indicated that the maximal fluorescence of CFP-MEM followed the PtdIns(3,4,5)P_3 spike (n=ten macropinosomes). The difference between two maxima was significant (*P<0.005). (D) Strategy for identifying cup closure using low concentrations of FM4-64. The top row shows the relative fluorescence of plasma membrane and macropinosome membranes under observation conditions. Plasma membranes will remain fluorescent owing to exchange of FM4-64 with dye in the buffer. Macropinosome closure will limit the reservoir of free FM4-64 to that which is enclosed in the vacuole; hence, the macropinosome fluorescence will diminish faster than the plasma-membrane fluorescence. Cup closure can be identified as the point at which macropinosome fluorescence photobleaches faster than plasma-membrane fluorescence. (E) Photobleaching of FM4-64 in macropinosomes revealed the timing of cup closure relative to the PtdIns(3,4,5)P_3 spike. Macrophages expressing YFP-BtkPH were imaged in the presence of M-CSF and 1 μg/ml FM4-64. The top row shows phase-contrast images of the stages of macropinosome formation. The middle row shows the intensity of YFP-BtkPH. YFP-BtkPH fluorescence in the macropinosome increased at t=+20 seconds (relative to ruffle closure), indicative of the PtdIns(3,4,5)P_3 spike. The bottom row shows the intensity of FM4-64, which indicates the relative membrane densities in each pixel. FM4-64 fluorescence in the plasma membrane decreased continuously owing to photobleaching and depletion of dye from the buffer. FM4-64 fluorescence in the macropinosome increased during the curved stage then decreased gradually during the circular stage. Scale bar: 3 μm. Color bars indicate the signal intensities of YFP-BtkPH or FM4-64 in each image. (F) Plots of YFP-BtkPH signal intensity in the macropinosome region (black circles) and the entire cell (white circles) of C. Time 0 marks ruffle closure. (G) Intensity of macropinosome (MP):intensity of whole cell area (Cell) for YFP-BtkPH fluorescence (white circles) and FM4-64 fluorescence (black circles) of A. Relative FM4-64 fluorescence in the macropinosome increased during ruffle and cup closure, then decreased afterwards. The point at which the ratio began to decrease indicated cup closure. Comparing the two curves indicates that the PtdIns(3,4,5)P_3 spike occurred between ruffle closure (t=0 seconds) and cup closure (t=+100 seconds). (H) Intensity (MP):intensity (Cell) for FM4-64 fluorescence, relative to ruffle closure (t=0 seconds), the PtdIns(3,4,5)P_3 spike (spike), the maximum ratio (peak) and the end of the circular stage (end), indicated that cup closure followed the spike of PtdIns(3,4,5)P_3 (n=nine macropinosomes). *P<0.01, **P<0.005, ***P<0.001.

would photobleach faster than dye in exposed plasma membrane, because the supply of FM4-64 from the fluid in the macropinosome would be limited (Fig. 5D). Based on this idea, we identified the timing of cup closure as an inflection point in FM4-64 fluorescence. M-CSF and low concentrations of FM4-64 (1 μg/ml) were added to BM-macrophages expressing YFP-BtkPH. As expected, FM4-64 showed considerable photobleaching in the plasma membrane during the observation period (Fig. 5E). To track selective photobleaching in macropinosomes, we measured FM4-64 fluorescence in macropinocytic cups relative to FM4-64 fluorescence of the whole cell. The intensity of the whole cell area decreased with time (Fig. 5F, white circles), indicating constant photobleaching and depletion of FM4-64 from the buffer. By contrast, the intensity in the macropinosome increased until t=0 seconds, presumably due to membrane folding in ruffles, then decreased. Dividing the average intensity on the macropinosome by that of the whole cell area (Fig. 5G, black circles) indicated that the relative fluorescence increased on circular ruffles (t=0 seconds), stayed almost the same for 80 seconds (t=0 to 80 seconds), then increased again before beginning to decrease (t=100 seconds) when FM4-64 was selectively photobleached (supplementary material Fig. S1). That is, at low, but not high, concentrations of FM4-64, the rate of photobleaching in macropinosomes increased relative to the overall rate of photobleaching for the cell, indicating that the limited supply of FM4-64 in the closed macropinosome could no longer replenish the bleached FM4-64 in the macropinosome membrane (Fig. 5D). Comparing the YFP-BtkPH fluorescence with the FM4-64-fluorescence ratios (Fig. 5G) indicated that the PtdIns(3,4,5)P_3 spike preceded the peak of FM4-64 ratios. Measurements from multiple macropinocytic events indicated that the peak of FM4-64 ratios occurred 82±42 seconds after ruffle closure (supplementary material Table S1; Fig. 5H). Nine of the ten macropinosomes examined by this method showed similar patterns of FM4-64-ratio increase and decrease following the PtdIns(3,4,5)P_3 spike (supplementary material Table S1). When cells were exposed to fourfold higher concentrations of FM4-64, the rate of photobleaching in macropinosomes was reduced, indicating that the higher rate of photobleaching in 1 μg/ml FM4-64 resulted from depletion of dye in closed macropinosomes (supplementary material Fig. S1). In all cases, cup closure was completed before the motile

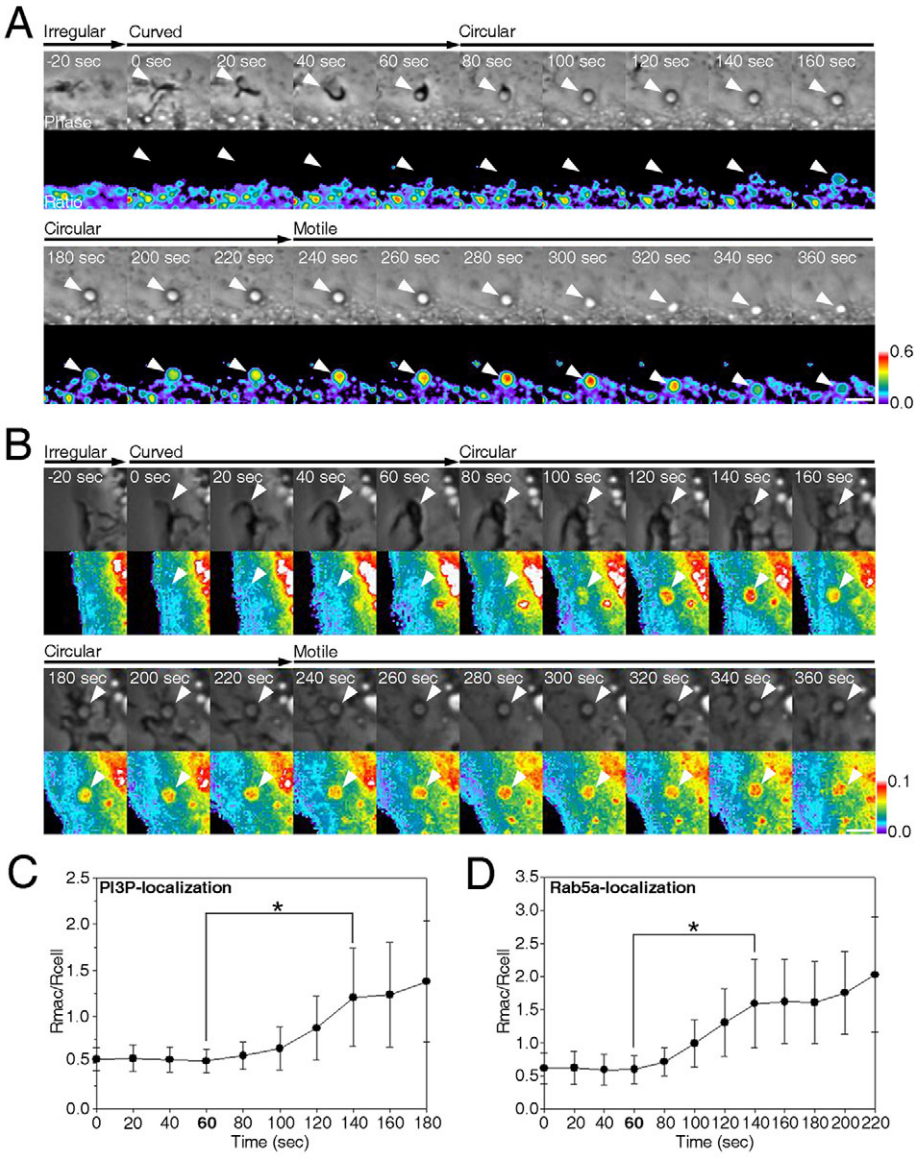

Fig. 6. PtdIns(3)*P* and Rab5a localization during macropinosome formation. (A) Phase-contrast (Phase) and ratiometric (Ratio) images of macropinosome formation in BM-macrophages expressing YFP-2×FYVE and CFP to localize PtdIns(3)*P* (PI3P). Indicated times are relative to the beginning of the curved-ruffle stage. Arrowhead indicates a forming macropinosome. Color bars indicate the molar ratio of YFP-2×FYVE:CFP in the ratio images. Scale bar: 3 μm. YFP-2×FYVE:CFP ratios increased after 140 seconds. (B) Ratiometric imaging of YFP-Rab5a localization during macropinosome formation in a BM-macrophage expressing YFP-Rab5a and CFP. '0 sec' marks the beginning of the curved-ruffle stage. Color bar indicates the molar ratio of YFP-Rab5a:CFP in the ratio images. Scale bar: 3 μm. The ratio of YFP-Rab5a:CFP increased on the macropinosome after 100 seconds. (C) Plots of average R_{mac}:R_{cell}, indicating the dynamics of YFP-2×FYVE on macropinosomes (n=10). 60 seconds marks the end of the curved-ruffle stage. YFP-2×FYVE localization continuously increased after 60 seconds. The difference between the localization index of YFP-2×FYVE at 60 and 140 seconds was significant (*P<0.005). Error bars indicate standard deviation. (D) Plots of average R_{mac}:R_{cell} indicate the dynamics of YFP-Rab5a localization to macropinosomes (n=10). Rab5a localization continuously increased after 60 seconds. The difference between the localization index of YFP-Rab5a at 60 and 140 seconds was significant (*P<0.005). Error bars indicate standard deviation.

stage. Taken together, these measurements place the PtdIns(3,4,5)P_3 spike after ruffle closure and well before cup closure.

Rab5a and PtdIns(3)*P* are recruited at cup closure

To analyze PtdIns(3)*P* distributions during macropinocytosis, we imaged YFP-2×FYVE and CFP in M-CSF-stimulated cells. The ratio images showed no increase until the circular stage, when R_{mac}:R_{cell} increased gradually (Fig. 6A). The tracking of ten events showed that PtdIns(3)*P* localization to macropinosomes reached significantly elevated levels by 140 seconds (80 seconds after ruffle closure) (Fig. 6C; supplementary material Table S1), suggesting that PtdIns(3)*P* accumulation began at about the time of cup closure.

Because Rab5a is involved in macropinosome formation (Lanzetti et al., 2004) and interacts with EEA1 (Simonsen et al., 1998; Lawe et al., 2002), we expected that Rab5a appearance on macropinosomes would resemble PtdIns(3)*P* dynamics. Ratio images of YFP-Rab5a and CFP showed no recruitment to macropinocytic cups during the irregular and curved stages. However, ratios increased gradually, beginning in the circular stage (Fig. 6B), and quantitative analyses of ten image series showed that YFP-Rab5a localization increased significantly by 140 seconds (80 seconds after ruffle closure) (Fig. 6D), similar to, but slightly faster than, the localization of YFP–2×FYVE-domain. Thus, PtdIns(3)*P* and Rab5a began to accumulate on macropinosomes after the PtdIns(3,4,5)P_3 spike and possibly before cup closure. The variability in the timing of ruffle and cup closure prevented precise correlation of Rab5a and PtdIns(3)*P* signals with cup closure.

Contributions of PI3K to signaling in the cup

To examine the role of PI3K signaling in macropinosome formation, we measured signals in macropinocytic cups formed in the presence of the PI3K inhibitor LY294002. As reported previously (Araki et al., 1996), macrophages in LY294002 could ruffle and form circular cups in response to M-CSF, but those cups did not close into macropinosomes. Ratiometric microscopy showed considerable recruitment of YFP-PBD to ruffles and cups that were formed in LY294002-treated macrophages (Fig. 7A), indicating PI3K-independent activation of Rac1. Out of the 29 observed cups, 24 showed YFP-PBD recruitment. However, in contrast to uninhibited cells, YFP-PBD recruitment after LY294002 treatment did not appear as a transient spike, which suggests that PtdIns(3,4,5)P_3 might influence the activation or deactivation of Rac1. By contrast, YFP-Rab5a was not recruited to cups formed in LY294002-treated macrophages (Fig. 7A) (0/24 observed cups showed YFP-Rab5a recruitment), suggesting that Rab5a recruitment is dependent on PtdIns(3,4,5)P_3 generation in cups.

In the absence of PI3K inhibitors, cups sometimes failed to close into macropinosomes. In such rare events, we observed recruitment of YFP-PBD in irregular patterns of association with cups and little or no recruitment of YFP-BtkPH (Fig. 7B). YFP-Rab5a was never recruited to those cups that failed to close (data not shown). Together, these observations of the rare cups that formed but failed to close indicate that PI3K activity is not required for Rac1 activation but is required for Rab5a recruitment to cups.

Discussion

By quantifying signal magnitudes and timing relative to morphological stages of macropinosome formation, this study identified a sequence of distinct signals occurring in a restricted domain of plasma membrane. Macrophages incubated overnight in medium lacking M-CSF responded to the addition of M-CSF with pronounced ruffling and spreading. Ruffles and lamellipodia in those cells contained active Cdc42 and Rac1, and high concentrations of PtdIns(3,4,5)P_3. However, after the first several minutes, cell-surface ruffling continued without those signals. Instead, PtdIns(3,4,5)P_3 and Rac1 signaling was restricted to sub-regions of the plasma membrane whose location was defined by ruffle closure. This indicates that M-CSF-receptor signal transduction is context-

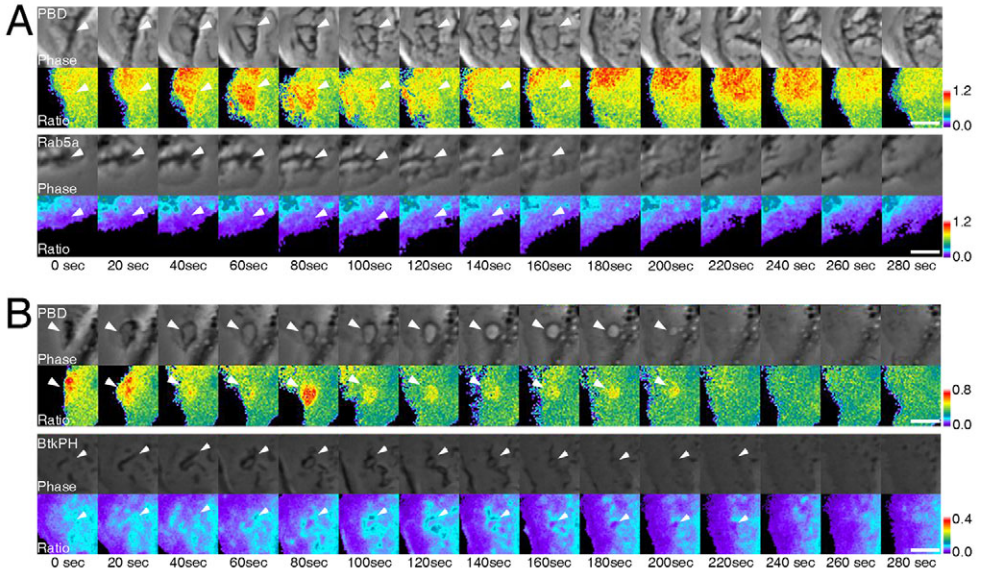

Fig. 7. Signaling on incompletely formed macropinosomes. (A) The effect of LY294002 on signaling in cups. Top two rows: phase-contrast (top) and YFP-PBD:CFP ratios (bottom) in macrophages treated with 50 µM LY294002 (30 minutes) then M-CSF. YFP-PBD was recruited to ruffles and cups, but the cups failed to close into macropinosomes. Bottom two rows: phase-contrast and YFP-Rab5a in LY294002-treated macrophages. YFP-Rab5a was not recruited to the cup. (B) Recruitment of YFP-PBD (top two rows) and YFP-BtkPH (bottom two rows) to cups, which failed to close into macropinosomes. YFP-PBD localized to the cup in an irregular temporal pattern. YFP-BtkPH did not localize to the cup. Arrowheads indicate a forming macropinosome. Scale bars: 3 µm.

dependent. That is, macropinosomes form stochastically at various times after addition of M-CSF. Once formation begins, the process continues through a sequence of morphological transitions consisting of two closure steps: ruffle closure and cup closure. The correlation reported here suggests that ruffle closure provides conditions that permit amplification of Rac1 and PtdIns(3,4,5)P_3 signaling in a restricted domain of the plasma membrane. Cup closure begins after the PtdIns(3,4,5)P_3 signal has decreased and after Rab5a, and possibly also PtdIns(3)*P*, appear in this sub-domain of the plasma membrane.

The morphological framework for macropinosome formation allowed correlation of signal-transduction events with distinct stages of macropinosome formation. In particular, four morphological stages of macropinocytosis were defined by time-lapse microscopy: irregular ruffles, curved ruffles, circular ruffles and motile macropinosomes. The timing of the transitions and the duration of the stages were highly variable and uncorrelated with each other. By studying a representative subset of macropinosomes, distinct correlations between morphology and phosphoinositide and small-GTPase signaling could be quantified. Two essential transitions were evident. First, activation of Rac1 and generation of PtdIns(3,4,5)P_3 increased immediately following ruffle closure, which suggests that a morphological condition is required for these signals. Early PI3K-independent Rac1 activation might initiate ruffling. Furthermore, the requirement of PI3K for macropinosome closure (Araki et al., 1996; Araki et al., 2006) indicates that the transition to circular ruffles permits PtdIns(3,4,5)P_3- and Rac1-dependent activities necessary for cup closure. Second, Rab5a localization and PtdIns(3)*P* generation increased slowly prior to cup closure, indicating that they too might contribute to cup closure (Fig. 8).

Earlier studies indicated that PtdIns(3)*P* appeared on macropinosomes after cup closure in A431 cells (Araki et al., 2007) and that type-III PI3K does not regulate macropinosome closure (Araki et al., 2006). The increase of PtdIns(3)*P* on macrophage macropinosomes was slightly slower than the recruitment of Rab5a. Owing to the variability of the timing of cup closure relative to ruffle closure, it is possible that the increase of PtdIns(3)*P* in macrophage macropinosomes begins after Rab5a recruitment and after cup closure. Further studies will examine the relative timing of Rab5a activation and PtdIns(3)*P* accumulation relative to cup closure.

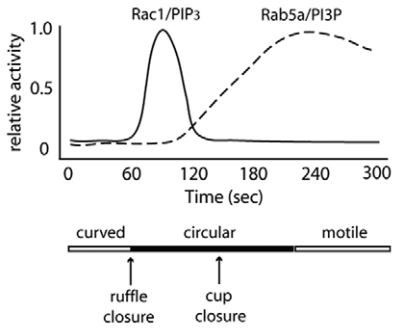

Fig. 8. Summary of the timing and relationship between morphology changes and signals during macropinosome formation. Graph shows the measured average times for the component activities. Independent of the time of addition of M-CSF, PtdIns(3,4,5)P_3 (PIP3) and Rac1 activities peaked shortly after ruffle closure. Deactivation of Rac1 and PtdIns(3,4,5)P_3 signals coincided with the appearance of Rab5a and PtdIns(3)*P* (PI3P). Recruitment of Rab5a, and possibly also PtdIns(3)*P*, to macropinocytic cups began prior to cup closure, which preceded the motile stage. The timing of the signals relative to the morphology suggests that the PtdIns(3,4,5)P_3-Rac1 spike requires ruffle closure and that the decrease of PtdIns(3,4,5)P_3 or the increase of PtdIns(3)*P* regulates cup closure.

The timing of the increase in CFP-MEM and FM4-64 fluorescence indicated that constriction of the distal cup rim for cup closure followed the PtdIns(3,4,5)P_3 spike and the increase in Rab5a and PtdIns(3)*P* (Figs 5 and 6). The role of the PtdIns(3,4,5)P_3 spike in cup closure is still unknown; however, because the spike was always observed after ruffle closure and before cup closure, this signal might organize cup closure. Because the PtdIns(3,4,5)P_3 spike is terminated long before cup closure, we speculate that PtdIns(3,4,5)P_3 localizes a secondary activity required for cup closure, such as the generation of diacylglycerol by phospholipase Cγ1 (Amyere et al., 2000). On the basis of light and electron microscopic observations, we suggest that two distinct steps organize cup closure: constriction at the distal margin of circular ruffles (evident in the increase in CFP-MEM and FM4-64 fluorescence) followed by a scission event that separates the macropinosome from the plasma membrane. Liberali et al. recently identified a role for C-terminal-binding protein-1/brefeldinA-ADP ribosylated substrate (CtBP1/BARS) in macropinosome scission (Liberali et al., 2008), which indicates a contribution of Rac1-dependent Pak-1 signaling in closure.

The mechanism by which cells switch from Rac1-PtdIns(3,4,5)P_3 signaling to Rab5a-PtdIns(3)*P* signaling is not known. Two proteins that could regulate the transition are Als2 (also known as alsin), a GEF for Rab5 and Rac1 (Topp et al., 2004; Topp et al., 2005), and SWAP-70, which binds activated Rac1 (Ihara et al., 2006) and associates transiently with macropinosomes in fibroblasts. Arf6 is another candidate molecule for regulating the transition from Rac1-PtdIns(3,4,5)P_3 to Rab5a-PtdIns(3)*P* on macropinosomes. Porat-Shliom et al. reported that macropinosome maturation in epithelial cells provides three distinct signaling platforms for the small GTPase H-Ras (Porat-Shliom et al., 2008). Expression of an active mutant of H-Ras, G12V, induced macropinocytosis. Live-cell imaging showed that, in H-Ras-G12V-expressing cells, incoming macropinosomes contained PtdIns(4,5)P_2 and PtdIns(3,4,5)P_3. Loss of PtdIns(4,5)P_2 from the macropinosomes was followed by the recruitment of Rab5, then PtdIns(3,4,5)P_3 was lost from the macropinosomes. Co-expression of an active mutant of Arf6, Q67L, inhibited Rab5 recruitment to H-Ras-G12V-induced macropinosomes, suggesting that Arf6 regulates Rab5 recruitment.

Taken together, the results demonstrate strong correlations between cell morphology and signal transduction during macropinosome formation. This indicates that morphology is not only a consequence of M-CSF signal transduction, but is also a contributing factor to feedback amplification and signal transitions. Thus, two new concepts are supported by these results: first, that signaling for macropinosome morphogenesis is contingent on the successful completion of ruffle closure and, second, that the contractile activities of cup closure might require a transition from Rac1-PtdIns(3,4,5)P_3 to Rab5a-PtdIns(3)*P*. Morphology-dependent signaling for macropinosome formation indicates that organelle morphogenesis is a self-organized, conditional progression of signals (Fig. 8). The signal modules are coordinated over micron-sized fields of membrane, which suggests that lateral diffusion integrates stages of signaling in sub-domains of the plasma membrane. What coordinates these activities spatially? M-CSF-receptor distribution seems unlikely, unless some presently unknown mechanism selectively concentrates receptors into macropinocytic

cups. We speculate that ruffle closure creates an isolated domain of plasma membrane, which permits amplification of PI3K activity. The rim of the circular ruffle might limit the diffusion of inner-leaflet phospholipids into or out of the circular ruffle, creating a confined domain of plasma membrane that permits the development of a positive-feedback loop involving PtdIns(3,4,5)P_3. Feedback systems involving Rac1 and PtdIns(3,4,5)P_3 have been implicated in ruffling and chemotaxis (Srinivasan et al., 2003; Papakonstanti et al., 2007). The subsequent decrease of PtdIns(3,4,5)P_3 or increase of diacylglycerol or PtdIns(3)P in the circular ruffle could stimulate contractile activities that constrict the distal margin of the circular ruffle, leading to cup closure.

Materials and Methods

Reagents

Recombinant mouse M-CSF was purchased from R&D Systems (Minneapolis, MN). FM4-64 and DMEM were from Invitrogen (Carlsbad, CA). RPMI1640 was from Lonza (Walkersville, MD). LY294002 was from EMD Chemicals (Gibbstown, NJ).

Cell culture

BM-macrophages were obtained as previously described (Swanson, 1989: Araki et al., 2003). Bone-marrow exudates obtained from femurs of female C57BL/6 mice (The Jackson Laboratory) were cultured in BM-macrophage medium (30% L-cell-conditioned medium as a source of M-CSF, 20% heat-inactivated fetal bovine serum, in DMEM) to promote growth and differentiation of macrophages. Cells were cultured at 37°C with 5% CO_2. At days 3 and 5, BM-macrophage-medium was added to the culture. At days 6 or 8, macrophages were harvested for transfection.

Plasmids and transfection

The plasmid pmCitrine-BtkPH-N1, which encodes YFP-BtkPH, was described previously (Kamen et al., 2007). mCitrine-Rab5a and pmCitrine-2×FYVE, which encode YFP-Rab5a and YFP-2×FYVE, respectively, were described previously (Henry et al., 2004), as were plasmids encoding YFP-Rac1, YFP-Rac2, YFP-Cdc42, YFP-PBD (p21-binding domain of Pak1), CFP and CFP-PBD (Hoppe and Swanson, 2004). The plasmid pECFP-Mem, encoding CFP-MEM, was purchased from Clontech. All plasmids were purified using an EndoFree Plasmid Purification kit (Qiagen). BM-macrophages were transfected with the plasmids by using Mouse Macrophage Nucleofector kit (Amaxa) according to the manufacturer's protocol. After transfection, cells were transferred to coverslips and incubated in RPMI-1640 with 20% HIFBS, 4 mM L-glutamine, 20 U/ml penicillin and 20 μg/ml streptomycin for 3 hours. Cells were incubated for 20 hours in DMEM without added M-CSF.

Fluorescence microscopy

Fluorescence images were collected using a Nikon Eclipse TE-300 inverted microscope with a 60× numerical aperture 1.4, oil-immersion PlanApo objective lens (Nikon, Tokyo, Japan) and a Lambda LS xenon arc lamp for epifluorescence illumination (Sutter Instruments, Novato, CA). Fluorescence excitation and emission wavelengths were selected using a JP4v2 filter set (Chroma Technology, Rockingham, VT) and a Lambda 10-2 filter wheel controller (Shutter Instruments) equipped with a shutter for epifluorescence illumination control. Images were recorded with a Photometrics CoolSnap HQ cooled CCD camera (Roper Scientific, Tucson, AZ). Image acquisition and processing were performed using MetaMorph v6.3 (Molecular Devices, Sunnyvale, CA).

Observation of macropinocytosis

Coverslips were assembled into Leiden chambers (Harvard Apparatus, Holliston, MA) at 37°C in Ringer's buffer (155 mM NaCl, 5 mM KCl, 2 mM $CaCl_2$, 1 mM $MgCl_2$, 2 mM NaH_2PO_4, 10 mM glucose and 10 mM HEPES at pH 7.2). Cells expressing fluorescent proteins were identified in the microscope, then M-CSF (200 ng/ml in Ringer's buffer) was added to stimulate ruffling and macropinocytosis. Immediately afterwards, time-lapse images were collected at 20-second or 3-second intervals for 30 minutes. The phase-contrast images were measured using MetaMorph to identify macropinosomes for analysis.

FRET microscopy

We used a method that measures FRET efficiency and the relative concentrations of donor, acceptor and donor-acceptor complexes inside cells (Hoppe et al., 2002). In a cell expressing YFP and CFP chimeras that can interact, such as Rac1-YFP and PBD-CFP, information about the stoichiometry of their interactions is contained in three images: I_D, the fluorescence from the donor, I_A, the fluorescence from the acceptor, and I_F, the mixture of donor, acceptor and FRET fluorescence. I_D, I_A and I_F were acquired by positioning excitation and emission filters to visualize CFP (excitation 435 nm, emission 490 nm), YFP (excitation 505 nm, emission 540 nm) and FRET (excitation 435 nm, emission 540 nm). Each image was then background-subtracted and shading-corrected (Hoppe et al., 2002). To account for different exposure times, image scaling was performed. The FRET parameters α and β were measured from COS-7 cells expressing only YFP or CFP, respectively. The parameters γ and ξ were determined using COS-7 cells expressing a linked CFP-YFP molecule, then the E_A, E_D, and R_M images were calculated from I_D, I_A and I_F using FRET stoichiometry equations as described previously (Hoppe et al., 2002; Beemiller et al., 2006).

Ratiometric imaging

A ratiometric imaging approach based on FRET stoichiometry was used to measure the molar ratios of two fluorescent chimeras in BM-macrophages (Hoppe et al., 2002; Beemiller et al., 2006). Ratio images reported the concentrations of YFP-chimera relative to CFP, thereby correcting for variations in optical path length related to cell shape. Using FRET stoichiometry, molar ratios of YFP-chimera to CFP (e.g. [YFP-Rab5a]/[CFP]) were calculated assuming there was no FRET (Hoppe et al., 2002; Beemiller et al., 2006). Alternatively, concentrations of PtdIns(3,4,5)P_3 on ruffles and macropinosomes were measured in cells expressing YFP-BtkPH and CFP-MEM, which normalized YFP fluorescence to distributions of membranes.

Macropinosome-tracking analysis

Particle-tracking analysis (Henry et al., 2004; Hoppe et al., 2004; Beemiller et al., 2006) was applied to macropinosomes in live cells. After identifying a macropinosome in a time-lapse sequence, its size at the end of the curved stage was measured. A region of interest (ROI) for each macropinosome was defined as a circle large enough to include the macropinocytosis event from the end of the irregular stage to the end of the motile stage. Signaling from multiple cellular events was measured by a particle-tracking image-analysis algorithm, developed using MetaMorph software, which tracked organelles or regions of an image in the phase-contrast image series by a cross-correlation centroid-tracking algorithm 'TRACOBJ' (Henry et al., 2004; Hoppe et al., 2004; Beemiller et al., 2006). The algorithm positioned the ROI in the computed images and the phase-contrast images at each frame in the time series. A threshold was applied over the cell and measurements were collected from a logical AND of the binary threshold and the grey-scale images, such that non-cellular regions (zeros) were not included in the computed averages. The tracking algorithm determined the center of the macropinosome region and then positioned the measurement region in the phase-contrast and ratio images (R_{mac}). A second region was drawn around the entire cell, then ratio values for the cell were measured (R_{cell}).

3D-reconstruction microscopy

Cells expressing YFP-BtkPH were incubated in medium containing FM4-64 (4 μg/ml). Imaging was performed on a custom-built, Nikon TE 2000 inverted microscope (Nikon, Tokyo, Japan) with a DG4 light source (Sutter Instruments, Novato, CA), two emCCD cameras (Cascade II, Roper Scientific, Tuscon, AZ) and filter wheels (Prior Scientific, Rockland, MA) (Hoppe et al., 2008). A 60× Plan Apo (violet corrected) water-immersion objective with a correction collar (Nikon, Tokyo, Japan) was used for imaging. Focus was controlled by moving this objective with a piezo controller (PIFOC; Physik Instruments, Kartsruhe, Germany) through z-axis steps of 0.2 μm.

After observation, deconvolution processing was carried out on each image using Huygens Essential (Scientific Volume Imaging, Hilversum, Netherlands). Resulting images were reconstructed to 3D images. To overlay images, deconvolved image planes were saved as TIFF files and processed in MetaMorph. A series of images along to z-direction at each time point were overlaid, and intensity of each signal was measured with the Linescan tool of MetaMorph.

Calculation of relative intensities of CFP-MEM in macropinosomes

In flat macrophages expressing CFP-MEM, fluorescence could be collected from labeled membranes of both the upper and lower surfaces of the cell. The total fluorescence in the region of the macropinosome increased as the curved ruffles closed into a distinct intracellular vacuole. A ratiometric method was used to quantify this increase in cells expressing variable amounts of CFP-MEM. The fluorescence intensity of CFP-MEM in the macropinosome region at the beginning of the curved stage represented the baseline fluorescence of plasma membrane. During macropinosome-tracking analysis, the fluorescence of the macropinosome region was divided by the baseline fluorescence to yield the relative fluorescence intensity at each time point. The time of maximal CFP-MEM fluorescence in the forming macropinosome indicated the point of cup closure.

Detection of macropinosome closure using FM4-64

The timing of cup closure was also measured using low concentrations of FM4-64 dye (1 μg/ml) included in the medium with M-CSF. Images were taken with a 555-nm excitation filter and a 605-nm emission filter.

Statistical analysis

A paired two-tailed Student's t-test was used to compare R_{mac}:R_{cell} values or FRET index values at different times. Pearson product-moment correlation coefficients and associated P-values were computed in MATLAB using the corrcoef.m function. The correlation coefficient can range from 1 to –1 (perfect correlation or anticorrelation) including 0 (no correlation).

This work was supported by NIH grants AI35950 and AI64668 to J.A.S. N.A. was supported by JSPS(590190). Deposited in PMC for release after 12 months.

References

Amyere, M., Payrastre, B., Krause, U., van der Smissen, P., Veithen, A. and Courtoy, P. J. (2000). Constitutive macropinocytosis in oncogene-transformed fibroblasts depends on sequential permanent activation phosphoinositide 3-kinase and phospholipase C. *Mol. Biol. Cell* **11**, 3453-3467.

Araki, N., Johnson, M. T. and Swanson, J. A. (1996). A role for phosphoinositide 3-kinase in the completion of macropinocytosis and phagocytosis by macrophages. *J. Cell Biol*. **135**, 1249-1260.

Araki, N., Hatae, T., Furukawa, A. and Swanson, J. A. (2003). Phosphoinositide-3-kinase-independent contractile activites associated with Fcγ-receptor-mediated phagocytosis and macropinocytosis in macrophages. *J. Cell Sci*. **116**, 247-257.

Araki, N., Hamasaki, M., Egami, Y. and Hatae, T. (2006). Effect of 3-methylamide on the fusion process of macropinosomes in EGF-stimulated A431 cells. *Cell Struct. Funct*. **31**, 145-157.

Araki, N., Egami, Y., Watanabe, Y. and Hatae, T. (2007). Phosphoinositide metabolism during membrane ruffling and macropinosome formation in EGF-stimulated A431 cells. *Exp. Cell Res*. **313**, 1496-1507.

Bar-Sagi, D. and Feramisco, J. R. (1986). Induction of membrane ruffling and fluid-phase pinocytosis in quiscent fibroblasts by *ras* proteins. *Science* **233**, 1061-1068.

Beemiller, P., Hoppe, A. D. and Swanson, J. A. (2006). A phosphatidylinositol-3-kinase-dependent signal transduction regulates ARF1 and ARF6 during Fcγ receptor-mediated phagocytosis. *PLoS Biol.* **4**, 0987-0999.

Cox, D., Chang, P., Zhang, Q., Reddy, P. G., Bokoch, G. M. and Greenberg, S. (1997). Requirement for both Rac1 and Cdc42 in membrane ruffling and phagocytosis in leukocytes. *J. Exp. Med.* **186**, 1487-1494.

Dharmawardhane, S., Schurmann, A., Sells, M. A., Chernoff, J., Schmid, S. L. and Bokoch, G. M. (2000). Regulation of macropinocytosis by p21-activated kinase-1. *Mol. Biol. Cell* **11**, 3341-3352.

Garrett, W. S., Chen, L. M., Kroschewski, R., Ebersold, M., Turley, S., Trombetta, S., Galan, J. E. and Mellman, I. (2000). Developmental control of endocytosis in Dendritic cells by Cdc42. *Cell* **102**, 325-334.

Gillooly, D. J., Morrow, I. C., Lindsay, M., Gould, R., Bryant, N. J., Gaullier, J. M., Parton, R. G. and Stenmark, H. (2000). Localization of phosphatidylinositol 3-phosphate in yeast and mammalian cells. *EMBO J.* **19**, 4577-4588.

Henry, R., Hoppe, A. D., Joshi, N. and Swanson, J. A. (2004). The uniformity of phagosome maturation in macrophages. *J. Cell Biol.* **164**, 185-194.

Hewlett, L. J., Prescott, A. R. and Watts, C. (1994). The coated pit and macropinocytic pathways serve distinct endosome populations. *J. Cell Biol.* **124**, 689-703.

Hoppe, A. D. and Swanson, J. A. (2004). Cdc42, Rac1, and Rac2 display distinct patterns of activation during phagocytosis. *Mol. Biol. Cell* **15**, 3509-3519.

Hoppe, A. D., Christensen, K. A. and Swanson, J. A. (2002). Fluorescence resonance energy transfer-based stoichiometry in living cells. *Biophys. J.* **83**, 3652-3664.

Hoppe, A. D., Shorte, S. L., Swanson, J. A. and Heintzmann, R. (2008). Three-dimensional FRET reconstruction microscopy for analysis of dynamic molecular interaction in live cells. *Biophys. J*. **95**, 400-418.

Ihara, S., Oka, T. and Fukui, Y. (2006). Direct binding of SWAP-70 to non-muscle actin is required for membrane ruffling. *J. Cell Sci.* **119**, 500-507.

Kamen, L. A., Levinsohn, J. and Swanson, J. A. (2007). Differential association of phosphatidylinositol 3-kinase, SHIP-1, and PTEN with forming phagosomes. *Mol. Biol. Cell* **18**, 2463-2472.

Katoh, H. and Negishi, H. (2003). RhoG activates Rac1 by direct interaction with Dock180-binding protein Elmo. *Nature* **424**, 461-464.

Kerr, M. C. and Teasdale, R. D. (2009). Defining macropinocytosis. *Traffic* **10**, 364-371.

Kheir, W. A., Gevrey, J.-C., Yamaguchi, H., Issac, B. and Cox, D. (2005). A WAVE2-Abi1 complex mediates CSF-1induced F-actin-rich membrane protrusions and migration in macrophage. *J. Cell Sci*. **118**, 5369-5379.

Kutateladze, T. G., Ogburn, K. D., Watson, W. T., de Beer, T., Emr, S. D., Burd, C. G. and Overduin, M. (1999). Phosphatidylinositol 3-phosphate recognition by the FYVE domain. *Mol. Cell* **3**, 805-811.

Lanzetti, L., Palamidessi, A., Areces, L., Scita, G. and DiFiore, P. P. (2004). Rab5 is a signaling GTPase involved in actin remodeling by receptor tyrosine kinases. *Nature* **429**, 309-314.

Lawe, D. C., Chawla, A., Merithew, E., Dumas, J., Carrington, W., Fogarty, K., Lifshiz, L., Tuft, R., Lambright, D. and Corvera, S. (2002). Sequential roles for phosphatidylinositol 3-phosphate and Rab5 in tethering and fusion of early endosomes via their interaction with EEA1. *J. Biol. Chem.* **277**, 8611-8617.

Li, G., D'Souza-Schorey, C., Barbieri, M. A., Cooper, J. A. and Stahl, P. D. (1997). Uncoupling of membrane ruffling and pinocytosis during Ras signal transduction. *J. Biol. Chem.* **272**, 10337-10340.

Liberali, P., Kakkonen, E., Turacchio, G., Valente, C., Spaar, A., Perinetti, G., Böckmann, R. A., Corda, D., Colanzi, A., Marjomaki, V. et al. (2008). The closure of Pak1-dependent macropinosomes requires the phosphorylation of CtBP1/BARS. *EMBO J.* **27**, 970-981.

Mercanti, V., Charette, S. J., Bennett, N., Ryckewaert, J. J., Letourneur, F. and Cosson, P. (2006). Selective membrane exclusion in phagocytic and macropinocytic cups. *J. Cell Sci.* **119**, 4079-4087.

Mercer, J. and Helenius, A. (2009). Virus entry by macropinocytosis. *Nat. Cell Biol.* **11**, 510-520.

Norbury, C. C. (2006). Drinking a lot is good for dendritic cells. *Immunology* **117**, 443-451.

Papaconstanti, E. A., Ridley, A. J. and Vanhaesebroeck, B. (2007). The p100 delta isoform of PI 3-kinase negatively controls RhoA and PTEN. *EMBO J.* **26**, 3050-3061.

Porat-Shliom, N., Kloog, Y. and Donaldson, J. G. (2008). A unique platform for H-Ras signaling involving clathrin-independent endocytosis. *Mol. Biol. Cell* **19**, 765-775.

Racoosin, E. L. and Swanson, J. A. (1989). Macrophage colony-stimulating factor (rM-CSF) stimulates pinocytosis in bone marrow-derived macrophages. *J. Exp. Med*. **170**, 1635-1648.

Schnatwinkel, C., Christoforidis, S., Lindsay, M. R., Uttenweiler-Joseph, S., Wilm, M., Parton, R. G. and Zerial, M. (2004). The Rab5 effector Rabankyrin-5 regulates and coordinates different endocytic mechanisms. *PLoS Biol.* **2**, 1363-1380.

Simonsen, A., Lippe, R., Christoforidis, S., Graullier, J. M., Brech, A., Callahan, J., Toh, B. H., Murphy, C., Zerial, M. and Stenmark, H. (1998). EEA1 links PI(3)K function to Rab5 regulation of endosome fusion. *Nature* **394**, 494-498.

Srinivasan, S., Wang, F., Glavas, S., Ott, A., Hofmann, F., Aktories, K., Kalman, D. and Bourne, H. R. (2003). Rac and Cdc42 play distinct roles in regulating $PI(3,4,5)P_3$ and polarity during neutrophil chemotaxis. *J. Cell Biol*. **160**, 375-385.

Swanson, J. A. (1989). Phorbol esters stimulate macropinocytosis and solute flow through macrophages. *J. Cell Sci.* **94**, 135-142.

Swanson, J. A. (2008). shaping cups into phagosomes and macropinosomes. *Nat. Rev. Mol. Cell Biol.* **9**, 639-649.

Topp, J. D., Gray, N. W., Gerard, R. D. and Horazdovsky, B. F. (2004). Alsin is a Rab5 and Rac1 guanine nucleotide exchange factor. *J. Biol. Chem*. **279**, 24612-24623.

Topp, J. D., Carney, D. S. and Horazdovsky, B. F. (2005). Biochemical characterization of Alsin, a Rab5 and Rac1 Guanine nucleotide Exchange Factor. *Methods Enzymol*. **403**, 261-276.

Varnai, P. and Balla, T. (1998). Visualization of phosphoinositides that bind pleckstrin homology domains: calcium- and agonist0induced dynamics and relationship to myo-[3H]inositol-labeled phosphoinositides pools. *J. Cell Biol.* **143**, 501-510.

Varnai, P., Rother, K. I. and Balla, T. (1999). Phosphatidylinositol 3-kinase-dependent membrane association of the Bruton's tyrosine kinase pleckstrin homology domain visualized in single living cells. *J. Biol. Chem.* **274**, 10983-10989.

Wells, C. M., Walmsley, M., Ooi, S., Tybulewicz, V. and Ridley, A. J. (2004). Rac1-deficient macrophages exhibit defects in cell spreading and membrane ruffling but not migration. *J. Cell Sci.* **117**, 1259-1268.

West, M. A., Prescott, A. R., Eskelinen, E. L., Ridley, A. J. and Watts, C. (2000). Rac is required for constitutive macropinocytosis by dendritic cells but does not control its downregulation. *Curr. Biol*. **10**, 839-848.

Zhang, Q., Calafat, J., Janssen, K. and Greenberg, S. (1999). ARF6 is required for growth factor- and Rac-mediated membrane ruffling in macrophages at a stage distal to Rac membrane targeting. *Mol. Cell. Biol*. **19**, 8158-8168.

Table S1. Summary of quantitation of the timing of signals and morphology during macropinosome formation

	1	2	3	4	5	6	7	8	9	10	Average	STDEV
Signal survey (10 standard)												
peak of Rac1-FRET	20	20	20	20	60	20	40	40	40	20	30	14.14
peak of BtkPH-Ratio	20	40	60	20	20	20	20	20	20	20	26	14
peak of Rab5a-Ratio	120	80	160	80	100	180	140	180	100	80	122	40.5
peak of 2xFYVE-Ratio	180	80	180	80	120	100	300	200	280	80	160	82.19
CFP-MEM experiment (4 standard+6)												
peak of CFP-MEM	100	100	100	100	80	20	80	80	120	100	88	27
beginning of motile	120	160	160	120	120	100	100	200	160	180	142	34.58
FM4-64 experiment (5standard+5)												
peak of FM4-64	160	100	100	20	100	100	100	40	60	40	82	41.58
beginning of motile	340	180	180	60	140	280	220	80	160	160	180	84.33
(t=0 is end of curved)												

Each value represents a separate experiment. Cup closure measurements (CFP-MEM experiment and FM4-64 experiment) were taken from a mixture of standard (60 second curved, 1.2-2.2 mm diameter) and non-standard (underlined) macropinosomes. Times are relative to ruffle closure (i.e. end of curved stage)